Carbohydrate Polymers 81 (2010) 484–490

Contents lists available at ScienceDirect

Carbohydrate Polymers

journal homepage: www.elsevier.com/locate/carbpol

Preparation and functional properties of blend films of gliadins and chitosan

Yinyong Li[a], Xiaolei Guo[a], Pengfei Lin[a], Congcheng Fan[a], Yihu Song[a,b,*]

[a] Department of Polymer Science and Engineering, Zhejiang University, Hangzhou 310027, China
[b] Key Laboratory of Macromolecular Synthesis and Functionalization of Ministry of Education, Zhejiang University, Hangzhou 310027, China

ARTICLE INFO

Article history:
Received 12 December 2009
Received in revised form 25 February 2010
Accepted 2 March 2010
Available online 9 March 2010

Keywords:
Film
Gliadins
Chitosan
Mechanical property
Morphology

ABSTRACT

This work was aimed to prepare wheat gliadin/chitosan (CS) blend films and to evaluate influence of CS content on properties of the films. Morphology observation using scanning electron microscope (SEM) revealed a phase-separated structure and a phase reversion with respect to CS content in the blend films. Dynamic mechanical analysis (DMA), differential scanning calorimetry (DSC) and Fourier transformation infrared (FTIR) spectrum measurements were conducted to assess the glass transition and microstructure of the films. Also studied were the mechanical properties and water barrier properties of the films. Results showed that gliadin/CS ratio had a significant effect on the functional performance of the films.

1. Introduction

Biopolymer-based films show promising potential as substitute of petroleum-based plastic package films to reduce environmental impact (Mangiacapra, Gorrasi, Sorrentino, & Vittoria, 2006; Mariniello et al., 2003; Rimdusit, Jingjid, Damrongsakkul, Tiptipakorn, & Takeichi, 2008; Yang, Yu, Feng, & Ma, 2007). Films prepared from wheat proteins, corn zein, gelatin, whey proteins, cellulose derivatives, chitosan, etc. (Arvanitoyannis, Psomiadou, & Nakayama, 1996; Bigi, Bracci, Cojazzi, Panzavolta, & Roveri, 1998; Limpisophon, Tanaka, Weng, Abe, & Osako, 2009) are generally biodegradable, nontoxic and edible and some of them are effective barriers to oxygen and carbon dioxide due to their tightly packed, ordered hydrogen-bonded network structure (Kester & Fennema, 1986; Yang & Paulson, 2000).

Edible films made from proteins usually show low mechanical strength, which limits their application (Zuo, Song, & Zheng, 2009). Crosslinking of proteins (Hernandez-Munoz, Villalobos, & Chiralt, 2004a; Larre, Desserme, Barbot, & Gueguen, 2000) is effective to enhance tensile and barrier properties (Kim, Sessa, & Lawton, 2004; Nuthong, Benjakul, & Prodpran, 2009; Park, Bae, & Rhee, 2000). Thermal treatment (Mangavel, Barbot, Popineau, & Gueguen, 2001) is able to promote crosslinking of proteins via disulphide bonding (Le Tien et al., 2000).

Chitosan (CS) is derived from chitin by deacetylation with alkali. Since chitin, obtained from fungal walls and exoskeletons of crustaceans and insects, is the second most abundant polysaccharide existing in nature (Chillo, Suriano, Lamacchia, & Del Nobile, 2009; Di Pierro et al., 2006; Jeon, Kamil, & Shahidi, 2002; Kittur, Kumar, & Tharanathan, 1998; Yoshida, Oliveira, & Franco, 2009), the source of chitosan is abundant and renewable (Mathew & Abraham, 2008; Zhuang & Liu, 2006). Films made from CS are nontoxic (Durango et al., 2006; Ferreira, Nunes, Delgadillo, & Lopes-da-Silva, 2009), biocompatible (Babiker, 2002; Ye, Neetoo, & Chen, 2008), antimicrobial (Alonso et al., 2009; Cagri, Ustunol, & Ryser, 2001; Fernandez-Saiz, Lagaron, Hemandez-Munoz, & Ocio, 2008, Fernandez-Saiz, Lagaron, & Ocio, 2009; Park & Bae, 2006; Pranoto, Rakshit, & Salokhe, 2005; Vasconez, Flores, Campos, Alvarado, & Gerschenson, 2009) and have good mechanical properties (Caner, Vergano, & Wiles, 1998; Hosokawa, Nishiyama, Yoshihara, & Kubo, 1990). Due to these excellent properties, CS has become a potential source for edible package film. Influences of degree of deacetylation of CS (Chang, Liu, Han, & Liu, 2008; Wiles, Vergano, Barron, Bunn, & Testin, 2000), plasticizers (Suyatma, Tighzert, & Copinet, 2005; Ziani, Oses, Coma, & Mate, 2008), fatty acids (Srinivasa, Ramesh, & Tharanathan, 2007), storage time (Butler, Vergano, Testin, Bunn, & Wiles, 1996) and condition (Fernandez-Saiz, Lagaron, & Ocio, 2009; Srinivasa, Ravi, & Tharanathan, 2007), crosslinkers (Mi et al., 2006; Shu & Zhu, 2002; Shu, Zhu, & Song, 2001), and enzyme (Kolodziejska & Piotrowska, 2007; Kolodziejska, Piotrowska, Bulge, & Tylingo, 2006; Sztuka & Kolodziejska, 2008) on properties of CS films have been studied. However, CS films usually show poor moisture barrier properties.

In order to obtain biodegradable films with better properties, composite films have been designed to combine the advantage of

---

* Corresponding author at: Department of Polymer Science and Engineering, Zhejiang University, Zheda Road No. 38, Hangzhou 310027, China.
Fax: +86 571 8795 3075.
E-mail address: s_yh0411@zju.edu.cn (Y. Song).

0144-8617/$ – see front matter © 2010 Elsevier Ltd. All rights reserved.
doi:10.1016/j.carbpol.2010.03.005

each component (Garcia, Pinotti, Martino, & Zaritzky, 2004). Combination of CS with soy protein (Silva, Santos, Coutinho, Mano, & Reis, 2005), whey protein (Di Pierro et al., 2006), ovalbumin (Di Pierro et al., 2007), silk fibroin (Chen, Li, Zhong, & Yu, 1997; Chen, Li, Shao, Zhong, & Yu, 1999; Du, Zhu, Chen, & Xu, 2006; Kim & Kim, 2005; Kweon, Ha, Um, & Park, 2001; Kweon, Um, & Park, 2001; Niamsa, Srisuwan, Baimark, Phinyocheep, & Kittipoom, 2009; Rujiravanit, Kruaykitanon, Jamieson, & Tokura, 2003) and keratin (Tanabe, Okitsu, Tachibana, & Yamauchi, 2002) have been investigated to prepare film with improved properties. Wheat gliadins have good viscoelastic properties (Song, Li, & Zheng, 2009a) and perfect film forming ability (Song, Jianrui, & Zheng, 2009). The objective of this work is to prepare gliadin/CS blend films combining good properties of both components. Influence of gliadin/CS ratio on the structure and properties of the blend films are investigated.

2. Experimental

2.1. Materials

Wheat gluten with a protein content ≥75%, a starch content ≤10%, a moisture content ≤9.0%, a fat content ≤6.5%, a cellulose content ≤0.5% and an ash content ≤0.95% was purchased from Shanghai Wangwei Food Co. Ltd., China. Chitosan (CS) with a degree of deacetylation ≥80% was supplied by Sinopharm Chem. Reagent Co. Ltd., China. Glycerol and ethanol used were of analytical grade.

2.2. Preparation of blend films

One hundred grams of wheat gluten powder were suspended in 350 ml pure ethanol and 150 ml distilled water was transferred into the suspension under stirring. The mixture was magnetic stirred for 1 h and centrifuged at 3000 rpm for 15 min at 25 °C. The supernatant containing the gliadin-rich fraction was collected as the film forming solution. This method was different from the general way that crude wheat gluten was dispersed in 70% (v/v) aqueous ethanol and stirred for about 12 h to extract gliadins (Hernandez-Munoz et al., 2004a; Hernandez-Munoz, Villalobos, & Chiralt, 2004b; Song, Li, & Zheng, 2009b). Glycerol as plasticizer was added into the supernatant in a content of 20 g/100 g dry protein.

Two grams of CS were dispersed in 97 g water before 1 g acetic acid was added to the mixture under stirring to give a CS content of 2.0 wt%. By doing this, clotting of CS in acetic acid aqueous solution could be avoided. Glycerol plasticizer was added into the solution in a content of 20 g/100 g CS.

The gliadin solution and CS solution were mixed and stirred for 20 min. The weight content of CS, w_{CS}, defined as the weight ratio of CS to total weight of CS plus gliadins, was varied from 0 wt% to 100 wt%. The final solution was poured onto horizontal plastic dishes and dried at 25 °C. The dried films were carefully peeled off from the dishes and were preconditioned at 25 °C at 57.5% relative humidity (RH) for 3 days at least before testing.

2.3. Morphology observation

Samples stretched to break in tensile tests were used in morphology observation. A scanning electron microscope (SEM, SLR10N, FEI, EINdhoven, Netherlands) was applied to observe the morphology of the fracture surface coated with gold powder at 25 kV.

2.4. Fourier transformation infrared (FTIR) spectra measurement

Powder from predried film was mixed with potassium bromide in a ratio of 1:25 (w/w) under infrared lamp radiation and the mixture was pressed into a transparent disc. FTIR spectra were measured using FTIR spectrometer (VECTOR 22, Bruker Optik, GmbH, Ettlingen, Germany) with a resolution of 4 cm^{-1}.

2.5. Dynamic mechanical analysis (DMA)

DMA was performed at 1 Hz with a dynamic mechanical thermal analyzer (DMA 242, NETZSCH, Selb, Germany) using tensile mode at a heating rate of 3 °C min^{-1}. A small amount of dimethylsilicone oil was coated on the sample surface in order to eliminate moisture interchange between the sample and the surroundings. Storage modulus (E') and loss factor ($\tan\delta$) were recorded as a function of temperature (T) from −100 °C to 180 °C.

2.6. Differential scanning calorimetry (DSC)

A Q100 differential scanning calorimeter (TA Instruments-Waters LLC, USA) was applied to analyze glass transition of the samples under nitrogen atmosphere. Predried samples (5–10 mg) were heated from 30 °C to 180 °C at a rate of 10 °C min^{-1} at the first run to remove moisture from samples and cooled to 30 °C at a rate of 20 °C min^{-1}. The DSC trace from 30 °C to 180 °C was recorded at a rate of 10 °C min^{-1} during the second run.

2.7. Mechanical properties

The film samples were cut into strips of 40 mm long and 10 mm wide. A universal testing machine (CMT-4204, Shenzhen SANS Test Machine Co. Ltd., China) was used to evaluate Young's modulus (E), tensile strength (σ_b) and elongation percentage at break (ε_b) of the films with an extension rate of 10 mm min^{-1} at 57.5% RH at 25 °C. The result was evaluated as the mean of at least five samples for each product.

2.8. Moisture absorption (MA)

Specimens of 0.1–0.2 g were stored in an airtight desiccator containing phosphorus pentoxide for 1 week until constant weight. The predried samples were transferred into desiccators with saturated solution of sodium bromide (57.5% RH) and allowed to reach moisture equilibrium at 25 °C to constant weight. MA was evaluated on dry basis and was reported as the average of three replicates.

2.9. Water vapor permeability (WVP)

WVP of films was determined gravimetrically at 25 °C according to ASTM E96-80 (1983). Three specimens, cut from each preconditioned film, were sealed to glass test cups with an exposed area $A = 1.39 \times 10^{-4}$ m^2, containing anhydrous phosphorus pentoxide (0% RH). The cups were placed in airtight desiccators maintained at 57.5% RH with saturated solution of sodium bromide. WVP was determined according to $\text{WVP} = \Delta wH/A\,\Delta t\,\Delta p$ after steady-state condition was reached when the weight gain became constant over prescribed time interval (Letendre, D'Aprano, Lacroix, Salmieri, & St-Gelais, 2002). Here, Δw is the weight gain of the cup over time interval Δt, and Δp is the vapor pressure difference across the film (Zuo et al., 2009).

2.10. Statistical analyses

Statistical analyses were performed with OriginPro 7.50 software (OriginLab Co., Northampton, MA, USA). The data were expressed as the mean value ± standard deviation.

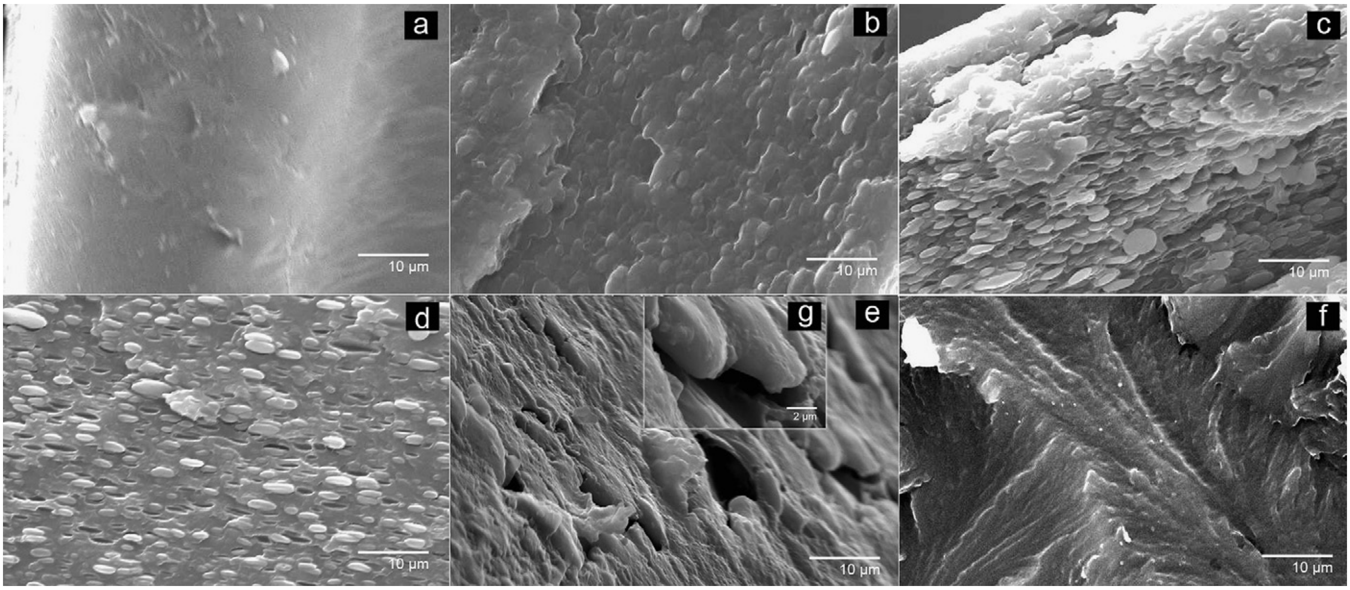

Fig. 1. SEM micrographs taken at the fracture surface of the films with w_{CS} of 0 wt% (a), 20 wt% (b), 40 wt% (c), 60 wt% (d), 80 wt% (e and g) and 100 wt% (f), respectively.

3. Results and discussion

3.1. Morphology of films

Fig. 1 shows SEM micrographs taken at the break surface of the films. Both the CS and the gliadin films are rather homogeneous and the CS film shows tough deformation characteristic with undulated fracture surface. In the film with w_{CS} = 80 wt%, the gliadins are distributed homogeneously in the CS component. Gliadin aggregated domain could not be recognized even at magnified micrograph (Fig. 1g). On the other hand, the blend films with w_{CS} of 20 wt%, 40 wt% and 60 wt% exhibit a phase-separated morphology containing ellipsoids with a long axis of about 3–4 μm and a short axis of about 1–2 μm dispersed in the continuous matrix. The ellipsoids are the most abundant at w_{CS} = 40 wt% where a phase reversion may occur as varying w_{CS}. The micrographs show that these particles of CS and gliadin have smooth surface.

3.2. FTIR spectra

Fig. 2 shows FTIR spectra of gliadin, CS and blend films. All these films exhibit a broad band in the region of 3700–3000 cm^{-1} related to O–H and N–H stretching vibration (Soares, Maia, Rayas-Duarte, & Soldi, 2009) as well as a group of bands in the region of 2800–3000 cm^{-1} assigned to C–H stretching vibrations (Secundo & Guerrieri, 2005). The absorption bands of gliadin film at about 1658 cm^{-1}, 1547 cm^{-1} and 1309 cm^{-1} are related to amide I (80% C=O stretch, 10% C–N stretch, and 10% N–H bend), amide II (60% N–H bend, 40% C–N stretch) and amide III (mixture of more than four components involving the amide group of the peptide chain), respectively (Robertson, Gregorski, & Cao, 2006). The absorbance of amide II band decreases considerably with increasing w_{CS}, which might be assigned to the intermolecular interaction between gliadin and CS. The main characteristic absorption bands of the chitosan film appear at 1631 cm^{-1} due to combination of the C=O stretching (amide I) and N–H bending (amide II) (Xu, Kim, Hanna, & Nag, 2005) and at 1405 cm^{-1} due to the C–N stretching (Qi, Xu, Jiang, Hu, & Zou, 2004). More specific bands of all these films falling in the 950–1200 cm^{-1} range might be attributed to C–O vibrations (Choudhari & Kariduraganavar, 2009; Secundo & Guerrieri, 2005; Shingel, 2002).

The amide III bands are suitable to judge the α-helix (1330–1295 cm^{-1}), β-turns (1295–1270 cm^{-1}), random coils (1270–1250 cm^{-1}) and β-sheets (1250–1220 cm^{-1}) structures (Cai & Singh, 1999; Song, Li, et al., 2009a). Fig. 3 shows the FTIR absorbance spectra in the amide III region. The gliadin film exhibits three marked peaks at 1309 cm^{-1}, 1274 cm^{-1}, and 1241 cm^{-1}, respectively while the CS film shows only one band at 1261 cm^{-1}. The 1309 cm^{-1} peak from gliadins shifts to 1311 cm^{-1} and 1317 cm^{-1} in the blend films with w_{CS} of 20 wt% and 60 wt%, respectively, and the half-peak width increases. The 1274 cm^{-1} peak disappears in the blend films, indicating the destruction of β-turns because of intermolecular interaction between gliadin and CS. The peak of CS at 1261 cm^{-1} and the peak of gliadin at 1241 cm^{-1} remain at the same positions while their areas decrease dramatically in the blend films. Therefore, the intermolecular interaction between gliadin and CS causes marked conformation changes in the α-helix, β-turns and β-sheets structures of gliadins.

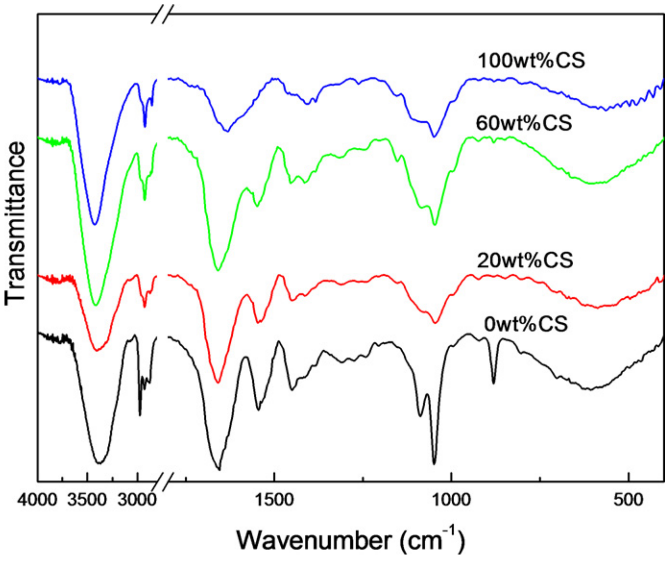

Fig. 2. FTIR spectra of the films.

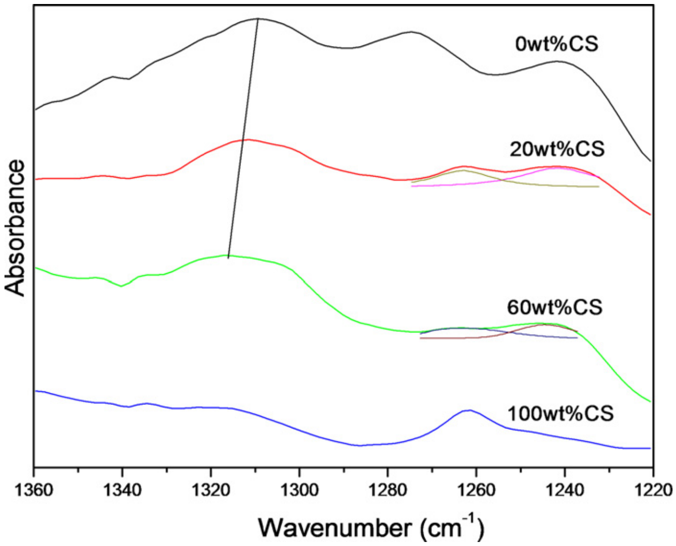

Fig. 3. FTIR absorbance spectra of the films in the amide III region.

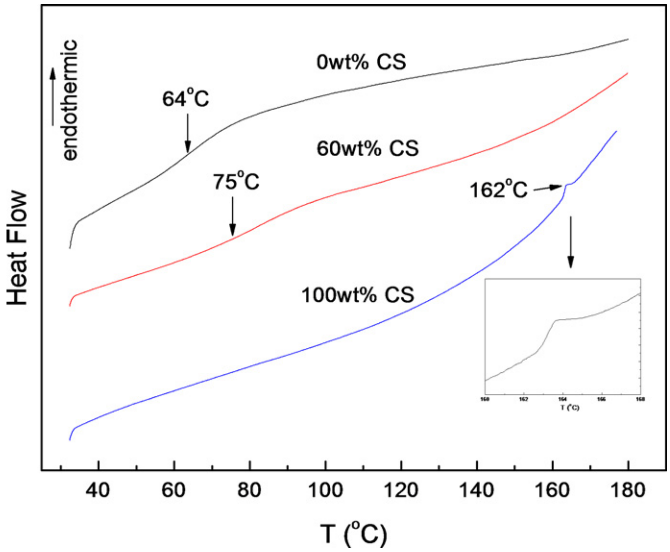

Fig. 5. DSC traces of gliadin film, blend film (w_{CS} = 60 wt%) and CS film.

3.3. Dynamical mechanical behavior

Fig. 4 shows E' and $\tan\delta$ as a function of T at frequency of 1 Hz. With increasing T, the gliadin films traverse the glassy, the wide glass-to-rubber transition ($\tan\delta$ peak and E' drop) and the rubbery plateau region in sequence. E' exhibits a value of 10^3–10^4 MPa in the glassy region while it decreases dramatically in the glassy transition region. E' of the blend films is much greater than gliadin film in the whole T range investigated.

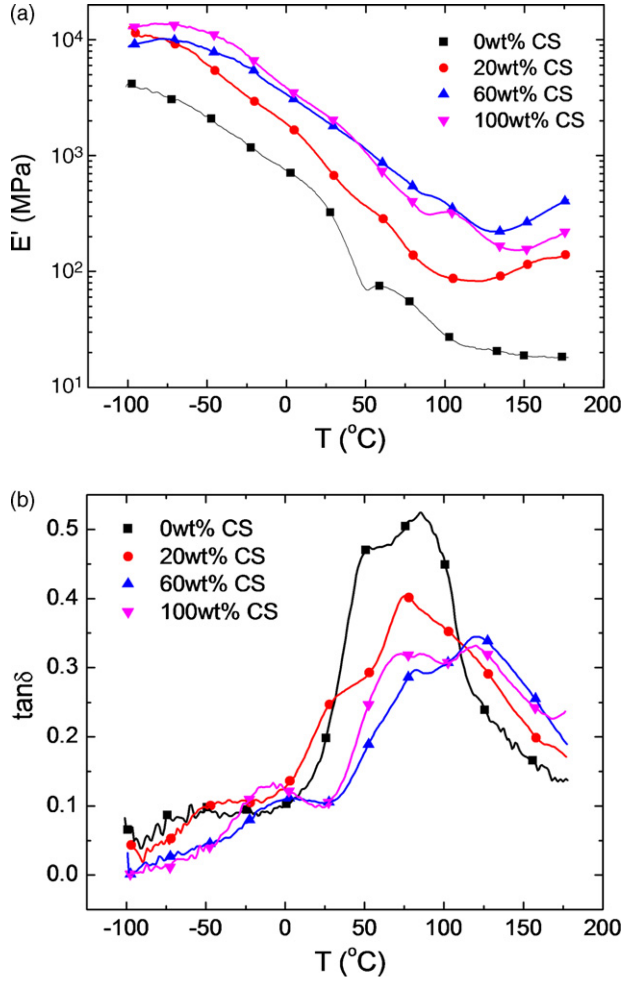

Fig. 4. Effect of w_{CS} on E' (a) and $\tan\delta$ (b) as a function of T for the films with different w_{CS}.

In the $\tan\delta$ curve, the gliadin film shows a broad transition from 0 °C to 100 °C, which is consistent with the sharp E' decay and is related to glass transition temperature (T_g) of plasticized gliadins (Song, Zheng, & Liu, 2008). The transition temperature is much lower than T_g of unplasticized gliadin at about 138 °C (Noel, Parker, Ring, & Tatham, 1995). In the rubbery plateau region, E' exhibits a tiny increase at 50 °C, which is consistent with the $\tan\delta$ shoulder peak in the T_g region and indicates the occurrence of sulphydryl-disulphide interchange reaction among gliadins during the DMA test (Song et al., 2009b). Since the crosslinking reaction among gliadins was not complete during the formation and storage of film, the thermal effect during the testing would accelerate the crosslinking reaction to a level which might overcome the thermally agitated softening effect, resulting a small increase of E' in the T_g region.

The CS film shows a large β relaxation between −50 °C and 20 °C, which associates to local motions of side groups in CS superposed on other non-identified transitions (Neto et al., 2005). This transition is absent in the blend films. In blend film with w_{CS} = 20 wt%, T_g of the glycerol-rich phase is hardly altered while the $\tan\delta$ value in the transition region from 30 °C to 110 °C is reduced considerably. The $\tan\delta$ curve of the blend film with w_{CS} = 60 wt% is very similar to the plasticized CS film, exhibiting two sub-transitions peaks at 75 °C and 120 °C, respectively, being much lower than T_g of unplasticized CS at 205 °C (Sakurai, Maegawa, & Takahashi, 2000). It is possible that the sub-transitions are related with CS-rich domains with different content of glycerol as well as water, due to different degree of plasticization. The complicated transition characteristic of the CS film could also be related to the reorganisation of packing of CS chains due to an increase of water mobility (Mucha & Pawlak, 2005) or to a local molecular motion in a pseudo-stable state in the presence of water (Sakurai et al., 2000).

3.4. Differential scanning calorimetry (DSC)

To check the influence of the absorbed water on the T_g determination from DMA, a heating–cooling treatment between 20 °C and 110 °C before recording DSC thermograms was performed. Fig. 5 shows the second running DSC traces of the gliadin film, the blend

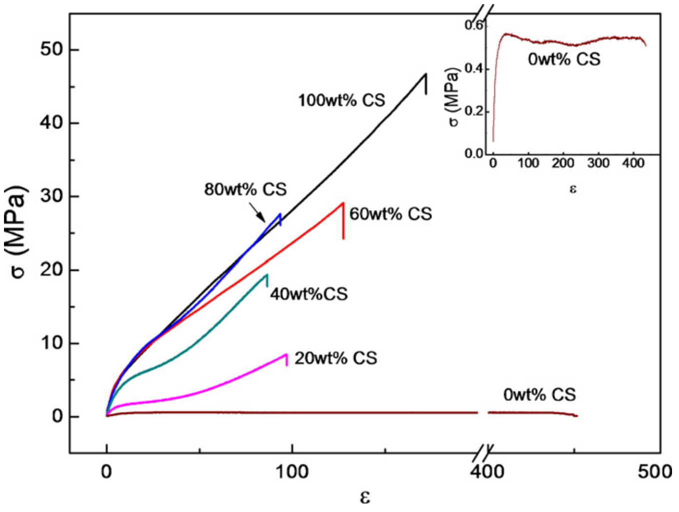

Fig. 6. Engineering stress–strain (σ–ε) relationship of the blend films at 57.5% RH.

film ($w_{CS} = 60$ wt%) and the CS film. The gliadin sample shows a glass transition at about 64 °C, which is located in the transition region in the tan δ curve in Fig. 4. A small transition area at the range of 160–170 °C observed on the DSC trace of the CS film corresponds to the glass transition of CS. The change of baseline in glass transition area is small because rigid CS is partial crystalline (Dong, Ruan, Wang, Zhao, & Bi, 2004; Sakurai et al., 2000). T_g of CS is estimated at about 162 °C at the heat flow jump, which is higher than the tan δ peak temperatures since the sample measured in DSC contains much less water. This value is much lower than T_g of unplasticized CS at 205 °C (Sakurai et al., 2000; Shantha & Harding, 2002) due to the plasticization effect of glycerol. T_g of gliadin in the blend film with $w_{CS} = 60$ wt% is determined at 75 °C. An increase of T_g of gliadins in the blend film might be assigned to the intermolecular interaction between gliadin and CS. However, the blend film does not show obvious glass transition of CS. A possible reason is that weak glass transition of CS in blend film is concealed by thermal effect of gliadins.

It is evident that absorbed water in the films gives rise to the different values of T_g evaluated from DMA and DSC tests. It is worth noting that, the complicated tan δ curve reflects a superposition crosslinking on glass transition of gliadins in the plasticized gliadin film. In the CS film, it reflects a superposition of glass relaxation on secondary relaxation of CS chains. In all the films, water loss undoubtedly occurs during DAM test, introducing another factor influencing E' and tan δ at high temperatures.

3.5. Mechanical properties

Mechanical properties of blend films are studied at 57.5% RH. Fig. 6 shows engineering stress–strain (σ–ε) relationship of the films. The gliadin film exhibits yielding at about $\varepsilon = 25\%$. After a small stress drop, the gliadin film undergoes a wide range of stress plateau until break. The CS film and the blend films do not exhibit stress drop and stress plateau upon stretching. σ of blend films increases more rapidly at small strains ($\varepsilon < 10\%$) than after yielding ($\varepsilon > 10\%$). For the CS film, σ increases almost linearly in the postyielding deformation.

Table 1 shows E, σ_b and ε_b of films. E and σ_b increase significantly ($p < 0.05$) with increasing w_{CS}, by about 15 and 47 times, respectively, as w_{CS} increasing from 0 wt% to 80 wt%. E and σ_b of the CS film are much higher than the gliadin film ($p < 0.05$) because of the stronger intermolecular interaction of CS. The blend films have a mechanical behavior between those of pure gliadins and CS films. At low w_{CS}, the CS particles in blend film, as shown in Fig. 1, may act as fillers to contribute hydrodynamic effect, which, together with the gliadin–CS interfacial intermolecular interaction, as shown in Fig. 3, might account for the improvements of E and σ_b of the blend films over the gliadin film. The blend films demonstrate a decrease in ε_b in comparison with both CS film and gliadin film ($p < 0.05$). The degeneration of extensibility might be related to island-sea structure in the blend film. Furthermore, the intermolecular interaction between gliadin and CS restricts the molecular motion of both macromolecules, which might be another reason for the reduction of ε_b in blend films. It is interesting that E, σ_b and ε_b increase simultaneously with increasing w_{CS} from 60 wt% to 100 wt%, which could be assigned to the phase-separated structure with CS as the continuous phase and the existence of strong interfacial interaction.

Table 1
Influence of w_{CS} on E, σ_b and ε_b of blend films at 57.5% RH[a].

w_{CS} (wt%)	E (MPa)	σ_b (MPa)	ε_b (%)
0	10.3 ± 0.6	0.61 ± 0.03	410 ± 42
20	41.9 ± 3.0	8.46 ± 0.71	101 ± 5
40	90.1 ± 7.1	18.86 ± 1.13	92 ± 5
60	127.8 ± 12.2	26.51 ± 0.94	91 ± 11
80	164.3 ± 11.1	29.27 ± 1.37	128 ± 7
100	214.1 ± 13.0	44.59 ± 4.59	177 ± 10

[a] Each value is the mean ± SD over at least five samples.

3.6. WVP and MA

Fig. 7 shows WVP and MA as a function of w_{CS}. Both WVP and MA increase with increasing w_{CS} ($p < 0.05$). The WVP value of the gliadin films is comparable to those of crosslinked gliadin and glutenin films ($2–6 \times 10^{-11}$ g m^{-1} s^{-1} Pa^{-1} at 50–54% RH; 25–33 wt% glycerol) (Hernandez-Munoz, Kanavouras, Ng, & Gavara, 2003; Hernandez-Munoz, Lopez-Rubio, Del-Valle, Almenar, & Gavara, 2004; Hernandez-Munoz et al., 2004a). The WVP value of the CS film at about 9.6×10^{-11} g m^{-1} s^{-1} Pa^{-1} in this study is close to that of glycerol plasticized CS film (9.1×10^{-11} g m^{-1} s^{-1} Pa^{-1}) but is lower than that of the unplasticized CS film (15.3×10^{-11} g m^{-1} s^{-1} Pa^{-1}) at 90% RH, due to formation of hydrogen bond between plasticizer and CS in the crevices of CS chains (Srinivasa, Ramesh, et al., 2007). Specifically, WVP of blend films with w_{CS} from 20 wt% to 60 wt% does not change much markedly, which might be related to the stack of the phase-separated ellipsoids in the continuous phase. The stack of the ellipsoids leads to an increased tortuous distance for water molecule diffusion in the blend film. On the other hand, the blend film with $w_{CS} = 80$ wt% does not exhibit phase separation

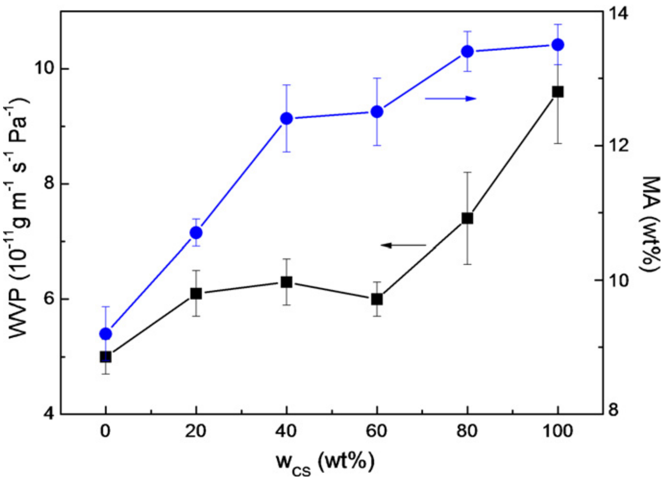

Fig. 7. Influence of w_{CS} on WVP and MA of the blend films.

so that the WVP value is considerably higher than those at w_{CS} from 20 wt% to 60 wt%.

Comparing with gliadin film and chitosan film, the blend films show advantages in several aspects. The blend films exhibit WVP and MA values lower than those of the CS film while their E, σ_b and E' are much higher than the gliadin film. Blending is therefore effective to enhance mechanical properties of gliadin film and moisture barrier properties of CS film. Moreover, the blends are expected to show good antimicrobial properties (Fernandez-Saiz et al., 2008), which may serve as antimicrobial packaging and coating to delay or prevent growth of microorganisms (Mayachiew, Devahastin, Mackey, & Niranjan, 2010). Antimicrobial films will be a major focus of functional food packaging in the future (Li, Kennedy, Peng, Yie, & Xie, 2006). As usual, it is permitted for antimicrobial films to contain higher concentrations of antimicrobial agents than that is allowed in food (Shen, Wu, Chen, & Zhao, 2010). When packaged with antimicrobial film, the surface of food has a high concentration of antimicrobial agents released gradually from the film while the actual concentration of antimicrobial agents in the whole food remains at a low level, which extends shelf-life of food and decreases the influence of antimicrobial agents on food as well (Pranoto et al., 2005). Because such edible films have shown potential effects on increasing the storage time and improving the quality of foods, such as meat, seafood, fruits and vegetables, by decreasing moisture and flavors loss, retarding oxidation, discoloration and decomposition (Gennadios, Hanna, & Kurth, 1997; Park, 1999), this kind of blend film has promising application in the packaging industry, either as edible food coatings or film wraps and pouches. Further researches should be performed to investigate the antimicrobial properties of the blend films. It is also important to improve the overall properties of the blend films and to reduce the production costs for obtaining efficient and more industrially accessible active antimicrobial systems.

4. Conclusion

The gliadin/CS ratio greatly affects the structure and performance of the blend films. The blend films with w_{CS} from 20 wt% to 60 wt% exhibited marked phase separation with formation of ellipsoids dispersed in the continuous phase. The present of CS leads to an increase in T_g of the gliadin-rich phase and a decrease in $\tan\delta$ in the transition region. There is some intermolecular interaction between gliadin and CS, which influences the conformation of gliadins in the blend films. E, σ_b, WVP and MA increase greatly with increasing w_{CS} while ε_b shows minimum at w_{CS} from 40 wt% to 60 wt%. Considering the antimicrobial properties of the CS component, the blend films are expected to serve as antimicrobial packaging and coating for foods.

Acknowledgements

This work was supported by National Natural Science Foundation of China (50773068) and Natural Science Foundation of Zhejiang Province (Y407011).

References

Alonso, D., Gimeno, M., Olayo, R., Vazquez-Torres, H., Sepulveda-Sanchez, J. D., & Shirai, K. (2009). Cross-linking chitosan into UV-irradiated cellulose fibers for the preparation of antimicrobial-finished textiles. *Carbohydrate Polymers*, *77*, 536–543.

Arvanitoyannis, I., Psomiadou, E., & Nakayama, A. (1996). Edible films made from sodium caseinate, starches, sugars or glycerol. 1. *Carbohydrate Polymers*, *31*, 179–192.

Babiker, E. E. (2002). Effect of chitosan conjugation on the functional properties and bactericidal activity of gluten peptides. *Food Chemistry*, *79*, 367–372.

Bigi, A., Bracci, B., Cojazzi, G., Panzavolta, S., & Roveri, N. (1998). Drawn gelatin films with improved mechanical properties. *Biomaterials*, *19*, 2335–2340.

Butler, B. L., Vergano, P. J., Testin, R. F., Bunn, J. M., & Wiles, J. L. (1996). Mechanical and barrier properties of edible chitosan films as affected by composition and storage. *Journal of Food Science*, *61*, 953–958.

Cagri, A., Ustunol, Z., & Ryser, E. T. (2001). Antimicrobial, mechanical, and moisture barrier properties of low pH whey protein-based edible films containing p-aminobenzoic or sorbic acids. *Journal of Food Science*, *66*, 865–870.

Cai, S. W., & Singh, B. R. (1999). Identification of beta-turn and random coil amide III infrared bands for secondary structure estimation of proteins. *Biophysical Chemistry*, *80*, 7–20.

Caner, C., Vergano, P. J., & Wiles, J. L. (1998). Chitosan film mechanical and permeation properties as affected by acid, plasticizer, and storage. *Journal of Food Science*, *63*, 1049–1053.

Chang, J, Liu, W. S., Han, B. Q., & Liu, B. (2008). Biological properties of chitosan films with different degree of deacetylation. *Journal of Materials Science & Technology*, *24*, 700–708.

Chen, X., Li, W. J., Shao, Z. Z., Zhong, W., & Yu, T. Y. (1999). Separation of alcohol-water mixture by pervaporation through a novel natural polymer blend membrane-chitosan/silk fibroin blend membrane. *Journal of Applied Polymer Science*, *73*, 975–980.

Chen, X., Li, W. J., Zhong, W., & Yu, T. Y. (1997). The Al^{3+} sensitivity of chitosan–silk fibroin complex membrane on swelling and its application on chemical valve for the separation of isopropanol–water mixture. *Journal of Macromolecular Science: Pure and Applied Chemistry A*, *34*, 2451–2460.

Chillo, S., Suriano, N., Lamacchia, C., & Del Nobile, M. A. (2009). Effects of additives on the rheological and mechanical properties of non-conventional fresh handmade tagliatelle. *Journal of Cereal Science*, *49*, 163–170.

Choudhari, S. K., & Kariduraganavar, M. Y. (2009). Development of novel composite membranes using quaternized chitosan and Na^+-MMT clay for the pervaporation dehydration of isopropanol. *Journal of Colloid and Interface Science*, *338*, 111–120.

Di Pierro, P., Chico, B., Villalonga, R., Mariniello, L., Damiao, A. E., Masi, P., et al. (2006). Chitosan–whey protein edible films produced in the absence or presence of transglutaminase: Analysis of their mechanical and barrier properties. *Biomacromolecules*, *7*, 744–749.

Di Pierro, P., Chico, B., Villalonga, R., Mariniello, L., Masi, P., & Porta, R. (2007). Transglutaminase-catalyzed preparation of chitosan–ovalbumin films. *Enzyme and Microbial Technology*, *40*, 437–441.

Dong, Y. M., Ruan, Y. H., Wang, H. W., Zhao, Y. G., & Bi, D. X. (2004). Studies on glass transition temperature of chitosan with four techniques. *Journal of Applied Polymer Science*, *93*, 1553–1558.

Du, C. H., Zhu, B. K., Chen, J. Y., & Xu, Y. Y. (2006). Metal ion permeation properties of silk fibroin/chitosan blend membranes. *Polymer International*, *55*, 377–382.

Durango, A. M., Soares, N. F. F., Benevides, S., Teixeira, J., Carvalho, M., Wobeto, C., et al. (2006). Development and evaluation of an edible antimicrobial film based on yam starch and chitosan. *Packaging Technology and Science*, *19*, 55–59.

Fernandez-Saiz, P., Lagaron, J. M., Hemandez-Munoz, P., & Ocio, M. J. (2008). Characterization of antimicrobial properties on the growth of *S. aureus* of novel renewable blends of gliadins and chitosan of interest in food packaging and coating applications. *International Journal of Food Microbiology*, *124*, 13–20.

Fernandez-Saiz, P., Lagaron, J. M., & Ocio, M. J. (2009a). Optimization of the biocide properties of chitosan for its application in the design of active films of interest in the food area. *Food Hydrocolloids*, *23*, 913–921.

Fernandez-Saiz, P., Lagaron, J. M., & Ocio, M. J. (2009b). Optimization of the film-forming and storage conditions of chitosan as an antimicrobial agent. *Journal of Agricultural and Food Chemistry*, *57*, 3298–3307.

Ferreira, C. O., Nunes, C. A., Delgadillo, I., & Lopes-da-Silva, J. A. (2009). Characterization of chitosan–whey protein films at acid pH. *Food Research International*, *42*, 807–813.

Garcia, M. A., Pinotti, A., Martino, M. N., & Zaritzky, N. E. (2004). Characterization of composite hydrocolloid films. *Carbohydrate Polymers*, *56*, 339–345.

Gennadios, A., Hanna, M. A., & Kurth, L. B. (1997). Application of edible coatings on meats, poultry and seafoods: A review. *Lebensmittel-Wissenschaft und-Technologie*, *30*, 337–350.

Hernandez-Munoz, P., Kanavouras, A., Ng, P. K. W., & Gavara, R. (2003). Development and characterization of biodegradable films made from wheat gluten protein fractions. *Journal of Agricultural and Food Chemistry*, *51*, 7647–7654.

Hernandez-Munoz, P., Lopez-Rubio, A., Del-Valle, V., Almenar, E., & Gavara, R. (2004). Mechanical and water barrier properties of glutenin films influenced by storage time. *Journal of Agricultural and Food Chemistry*, *52*, 79–83.

Hernandez-Munoz, P., Villalobos, R., & Chiralt, A. (2004a). Effect of cross-linking using aldehydes on properties of glutenin-rich films. *Food Hydrocolloids*, *18*, 403–411.

Hernandez-Munoz, P., Villalobos, R., & Chiralt, A. (2004b). Effect of thermal treatments on functional properties of edible films made from wheat gluten fractions. *Food Hydrocolloids*, *18*, 647–654.

Hosokawa, J., Nishiyama, M., Yoshihara, K., & Kubo, T. (1990). Biodegradable film derived from chitosan and homogenized cellulose. *Industrial & Engineering Chemistry Research*, *29*, 800–805.

Jeon, Y. J., Kamil, J. Y. V. A., & Shahidi, F. (2002). Chitosan as an edible invisible film for quality preservation of herring and Atlantic cod. *Journal of Agricultural and Food Chemistry*, *50*, 5167–5178.

Kester, J. J., & Fennema, O. R. (1986). Edible films and coatings—a review. *Food Technology*, *40*, 47–59.

Kim, D. K., & Kim, H. S. (2005). Structure and characteristic of chitosan Bombyx mori silk fibroin blend films. *Polymer-Korea*, *29*, 408–412.

Kim, S., Sessa, D. J., & Lawton, J. W. (2004). Characterization of zein modified with a mild cross-linking agent. *Industrial Crops and Products*, *20*, 291–300.

Kittur, F. S., Kumar, K. R., & Tharanathan, R. N. (1998). Functional packaging properties of chitosan films. *Zeitschrift Fur Lebensmittel-Untersuchung Und-Forschung A: Food Research and Technology*, *206*, 44–47.

Kolodziejska, I., & Piotrowska, B. (2007). The water vapour permeability, mechanical properties and solubility of fish gelatin–chitosan films modified with transglutaminase or 1-ethyl-3-(3-dimethylaminopropyl) carbodiimide (EDC) and plasticized with glycerol. *Food Chemistry*, *103*, 295–300.

Kolodziejska, I., Piotrowska, B., Bulge, M., & Tylingo, R. (2006). Effect of transglutaminase and 1-ethyl-3-(3-dimethylaminopropyl) carbodiimide on the solubility of fish gelatin-chitosan films. *Carbohydrate Polymers*, *65*, 404–409.

Kweon, H., Ha, H. C., Um, I. C., & Park, Y. H. (2001). Physical properties of silk fibroin/chitosan blend films. *Journal of Applied Polymer Science*, *80*, 928–934.

Kweon, H. Y., Um, I. C., & Park, Y. H. (2001). Structural and thermal characteristics of Antheraea pernyi silk fibron/chitosan blend film. *Polymer*, *42*, 6651–6656.

Larre, C., Desserme, C., Barbot, J., & Gueguen, J. (2000). Properties of deamidated gluten films enzymatically cross-linked. *Journal of Agricultural and Food Chemistry*, *48*, 5444–5449.

Le Tien, C., Letendre, M., Ispas-Szabo, P., Mateescu, M. A., Delmas-Patterson, G., Yu, H. L., et al. (2000). Development of biodegradable films from whey proteins by cross-linking and entrapment in cellulose. *Journal of Agricultural and Food Chemistry*, *48*, 5566–5575.

Letendre, M., D'Aprano, G., Lacroix, M., Salmieri, S., & St-Gelais, D. (2002). Physicochemical properties and bacterial resistance of biodegradable milk protein films containing agar and pectin. *Journal of Agricultural and Food Chemistry*, *50*, 6017–6022.

Li, B., Kennedy, J. F., Peng, J. L., Yie, X., & Xie, B. J. (2006). Preparation and performance evaluation of glucomannan–chitosan–nisin ternary antimicrobial blend film. *Carbohydrate Polymers*, *65*, 488–494.

Limpisophon, K., Tanaka, M., Weng, W. Y., Abe, S., & Osako, K. (2009). Characterization of gelatin films prepared from under-utilized blue shark (Prionace glauca) skin. *Food Hydrocolloids*, *23*, 1993–2000.

Mangavel, C., Barbot, J., Popineau, Y., & Gueguen, J. (2001). Evolution of wheat gliadins conformation during film formation: A Fourier transform infrared study. *Journal of Agricultural and Food Chemistry*, *49*, 867–872.

Mangiacapra, P., Gorrasi, G., Sorrentino, A., & Vittoria, V. (2006). Biodegradable nanocomposites obtained by ball milling of pectin and montmorillonites. *Carbohydrate Polymers*, *64*, 516–523.

Mariniello, L., Di Pierro, P., Esposito, C., Sorrentino, A., Masi, P., & Porta, R. (2003). Preparation and mechanical properties of edible pectin-soy flour films obtained in the absence or presence of transglutaminase. *Journal of Biotechnology*, *102*, 191–198.

Mathew, S., & Abraham, T. E. (2008). Characterisation of ferulic acid incorporated starch-chitosan blend films. *Food Hydrocolloids*, *22*, 826–835.

Mayachiew, P., Devahastin, S., Mackey, B. M., & Niranjan, K. (2010). Effects of drying methods and conditions on antimicrobial activity of edible chitosan films enriched with galangal extract. *Food Research International*, *43*, 125–132.

Mi, F. L., Huang, C. T., Liang, H. F., Chen, M. C., Chiu, Y. L., Chen, C. H., et al. (2006). Physicochemical, antimicrobial, and cytotoxic characteristics of a chitosan film cross-linked by a naturally occurring cross-linking agent, aglycone geniposidic acid. *Journal of Agricultural and Food Chemistry*, *54*, 3290–3296.

Mucha, M., & Pawlak, A. (2005). Thermal analysis of chitosan and its blends. *Thermochimica Acta*, *427*, 69–76.

Neto, C. G. T., Giacometti, J. A., Job, A. E., Ferreira, F. C., Fonseca, J. L. C., & Pereira, M. R. (2005). Thermal analysis of chitosan based networks. *Carbohydrate Polymers*, *62*, 97–103.

Niamsa, N., Srisuwan, Y., Baimark, Y., Phinyocheep, P., & Kittipoom, S. (2009). Preparation of nanocomposite chitosan/silk fibroin blend films containing nanopore structures. *Carbohydrate Polymers*, *78*, 60–65.

Noel, T. R., Parker, R., Ring, S. G., & Tatham, A. S. (1995). The glass-transition behavior of wheat gluten proteins. *International Journal of Biological Macromolecules*, *17*, 81–85.

Nuthong, P., Benjakul, S., & Prodpran, T. (2009). Characterization of porcine plasma protein-based films as affected by pretreatment and cross-linking agents. *International Journal of Biological Macromolecules*, *44*, 143–148.

Park, H. J. (1999). Development of advanced edible coatings for fruits. *Trends in Food Science & Technology*, *10*, 254–260.

Park, S. K., & Bae, D. H. (2006). Antimicrobial properties of wheat gluten–chitosan composite film in intermediate-moisture food systems. *Food Science and Biotechnology*, *15*, 133–137.

Park, S. K., Bae, D. H., & Rhee, K. C. (2000). Soy protein biopolymers cross-linked with glutaraldehyde. *Journal of the American Oil Chemists Society*, *77*, 879–883.

Pranoto, Y., Rakshit, S. K., & Salokhe, V. M. (2005). Enhancing antimicrobial activity of chitosan films by incorporating garlic oil, potassium sorbate and nisin. *LWT—Food Science and Technology*, *38*, 859–865.

Qi, L. F., Xu, Z. R., Jiang, X., Hu, C. H., & Zou, X. F. (2004). Preparation and antibacterial activity of chitosan nanoparticles. *Carbohydrate Research*, *339*, 2693–2700.

Rimdusit, S., Jingjid, S., Damrongsakkul, S., Tiptipakorn, S., & Takeichi, T. (2008). Biodegradability and property characterizations of methyl cellulose: Effect of nanocompositing and chemical crosslinking. *Carbohydrate Polymers*, *72*, 444–455.

Robertson, G. H., Gregorski, K. S., & Cao, T. K. (2006). Changes in secondary protein structures during mixing development of high absorption (90%) flour and water mixtures. *Cereal Chemistry*, *83*, 136–142.

Rujiravanit, R., Kruaykitanon, S., Jamieson, A. M., & Tokura, S. (2003). Preparation of crosslinked chitosan/silk fibroin blend films for drug delivery system. *Macromolecular Bioscience*, *3*, 604–611.

Sakurai, K., Maegawa, T., & Takahashi, T. (2000). Glass transition temperature of chitosan and miscibility of chitosan/poly(N-vinyl pyrrolidone) blends. *Polymer*, *41*, 7051–7056.

Secundo, F., & Guerrieri, N. (2005). ATR-FT/IR study on the interactions between gliadins and dextrin and their effects on protein secondary structure. *Journal of Agricultural and Food Chemistry*, *53*, 1757–1764.

Shantha, K. L., & Harding, D. R. K. (2002). Synthesis and characterisation of chemically modified chitosan microspheres. *Carbohydrate Polymers*, *48*, 247–253.

Shen, X. L., Wu, J. M., Chen, Y. H., & Zhao, G. H. (2010). Antimicrobial and physical properties of sweet potato starch films incorporated with potassium sorbate or chitosan. *Food Hydrocolloids*, *24*, 285–290.

Shingel, K. I. (2002). Determination of structural peculiarities of dexran, pullulan and gamma-irradiated pullulan by Fourier-transform IR spectroscopy. *Carbohydrate Research*, *337*, 1445–1451.

Shu, X. Z., & Zhu, K. J. (2002). The influence of multivalent phosphate structure on the properties of ionically cross-linked chitosan films for controlled drug release. *European Journal of Pharmaceutics and Biopharmaceutics*, *54*, 235–243.

Shu, X. Z., Zhu, K. J., & Song, W. H. (2001). Novel pH-sensitive citrate cross-linked chitosan film for drug controlled release. *International Journal of Pharmaceutics*, *212*, 19–28.

Silva, S. S., Santos, M. I., Coutinho, O. P., Mano, J. F., & Reis, R. L. (2005). Physical properties and biocompatibility of chitosan/soy blended membranes. *Journal of Materials Science: Materials in Medicine*, *16*, 575–579.

Soares, R. M. D., Maia, G. S., Rayas-Duarte, P., & Soldi, V. (2009). Properties of filmogenic solutions of gliadin crosslinked with 1-(3-dimethyl aminopropyl)-3-ethylcarbodiimidehydrochloride/N-hydroxysuccinimide and cysteine. *Food Hydrocolloids*, *23*, 181–187.

Song, Y., Zheng, Q., & Liu, C. (2008). Green biocomposites from wheat gluten and hydroxyethyl cellulose: Processing and properties. *Industrial Crops and Products*, *28*, 56–62.

Song, Y. H., Jianrui, C., & Zheng, Q. (2009). Influence of methylcellulose on dynamic rheology of dilute wheat gliadin solution in 50% (v/v) aqueous propanol. *Journal of Food Engineering*, *94*, 290–294.

Song, Y. H., Li, L. F., & Zheng, Q. (2009a). Influence of epichlorohydrin modification on structure and properties of wheat gliadin films. *Journal of Agricultural and Food Chemistry*, *57*, 2295–2301.

Song, Y. H., Li, L. F., & Zheng, Q. (2009b). Influence of methylcellulose on properties of wheat gliadin film cast from aqueous ethanol. *Food Science and Biotechnology*, *18*, 910–916.

Srinivasa, P. C., Ramesh, M. N., & Tharanathan, R. N. (2007). Effect of plasticizers and fatty acids on mechanical and permeability characteristics of chitosan films. *Food Hydrocolloids*, *21*, 1113–1122.

Srinivasa, P. C., Ravi, R., & Tharanathan, R. N. (2007). Effect of storage conditions on the tensile properties of eco-friendly chitosan films by response surface methodology. *Journal of Food Engineering*, *80*, 184–189.

Suyatma, N. E., Tighzert, L., & Copinet, A. (2005). Effects of hydrophilic plasticizers on mechanical, thermal, and surface properties of chitosan films. *Journal of Agricultural and Food Chemistry*, *53*, 3950–3957.

Sztuka, K., & Kolodziejska, I. (2008). Effect of transglutaminase and EDC on biodegradation of fish gelatin and gelatin–chitosan films. *European Food Research and Technology*, *226*, 1127–1133.

Tanabe, T., Okitsu, N., Tachibana, A., & Yamauchi, K. (2002). Preparation and characterization of keratin-chitosan composite film. *Biomaterials*, *23*, 817–825.

Vasconez, M. B., Flores, S. K., Campos, C. A., Alvarado, J., & Gerschenson, L. N. (2009). Antimicrobial activity and physical properties of chitosan–tapioca starch based edible films and coatings. *Food Research International*, *42*, 762–769.

Wiles, J. L., Vergano, P. J., Barron, F. H., Bunn, J. M., & Testin, R. F. (2000). Water vapor transmission rates and sorption behavior of chitosan films. *Journal of Food Science*, *65*, 1175–1179.

Xu, Y. X., Kim, K. M., Hanna, M. A., & Nag, D. (2005). Chitosan–starch composite film: Preparation and characterization. *Industrial Crops and Products*, *21*, 185–192.

Yang, J. H., Yu, J. G., Feng, Y., & Ma, X. F. (2007). Study on the properties of ethylenebisformamide plasticized corn starch (EPTPS) with various original water contents of corn starch. *Carbohydrate Polymers*, *69*, 256–261.

Yang, L., & Paulson, A. T. (2000). Mechanical and water vapour barrier properties of edible gellan films. *Food Research International*, *33*, 563–570.

Ye, M., Neetoo, H., & Chen, H. Q. (2008). Effectiveness of chitosan-coated plastic films incorporating antimicrobials in inhibition of Listeria monocytogenes on cold-smoked salmon. *International Journal of Food Microbiology*, *127*, 235–240.

Yoshida, C. M. P., Oliveira, E. N., & Franco, T. T. (2009). Chitosan tailor-made films: The effects of additives on barrier and mechanical properties. *Packaging Technology and Science*, *22*, 161–170.

Zhuang, X. P., & Liu, X. F. (2006). Blend films of O-carboxymethyl chitosan and cellulose in N-methylmorpholine-N-oxide monohydrate. *Journal of Applied Polymer Science*, *102*, 4601–4605.

Ziani, K., Oses, J., Coma, V., & Mate, J. I. (2008). Effect of the presence of glycerol and Tween 20 on the chemical and physical properties of films based on chitosan with different degree of deacetylation. *LWT—Food Science and Technology*, *41*, 2159–2165.

Zuo, M., Song, Y. H., & Zheng, Q. (2009). Preparation and properties of wheat gluten/methylcellulose binary blend film casting from aqueous ammonia: A comparison with compression molded composites. *Journal of Food Engineering*, *91*, 415–422.